Journal of Physiology (1995), **489.2**, *pp.*529–543

Dependence of the $GABA_A$ receptor gating kinetics on the α-subunit isoform: implications for structure–function relations and synaptic transmission

K. J. Gingrich*†, W. A. Roberts† and R. S. Kass*‡

**Department of Physiology and †Anesthesiology, University of Rochester, School of Medicine, 601 Elmwood Avenue, Rochester, NY 14642, USA*

1. To examine the dependence of γ-aminobutyric acid ($GABA_A$) receptor gating on the α-subunit isoform, we studied the kinetics of GABA-gated currents (I_{GABA}) of receptors that differed in the α-subunit subtype, $\alpha1\beta2\gamma2S$ and $\alpha3\beta2\gamma2S$. cDNAs encoding rat brain subunits were co-expressed heterologously in HEK-293 cells and the resultant receptors studied with the whole-cell patch clamp technique and rapidly applied GABA pulses (5–10 s).

2. I_{GABA} of both receptors showed a loosely similar dependence on GABA concentration over a wide range (1–5000 μM). Generally, I_{GABA} manifested activation reaching an early current peak, subsequent slower spontaneous desensitization, and deactivation of open channels at pulse termination. Lowering GABA concentrations reduced peak currents and slowed activation and desensitization kinetics.

3. The presence of $\alpha3$ altered the peak I_{GABA} concentration–response relationship by shifting the fitted Hill equation to tenfold greater GABA concentrations (GABA concentration at half amplitude: $\alpha1$, 7 μM; and $\alpha3$, 75 μM) without affecting Hill coefficients ($\alpha1$, 1·6; $\alpha3$, 1·5). These findings indicate a reduction in the apparent activating site affinity and are consistent with previous reports.

4. To investigate differences in gating, we normalized for apparent activating site affinities by analysing the time course of macroscopic gating at equi-activating GABA concentrations. The presence of $\alpha3$ slowed activation fourfold (time to current peak (means ± S.E.M.): $\alpha1$, 1·2 ± 0·06 s (2 μM); $\alpha3$, 4·7 ± 0·5 s (20 μM)), desensitization nearly twofold (reciprocal of time to 80% decay: $\alpha1$, 2·5 ± 0·48 s^{-1} (100 μM); $\alpha3$, 1·5 ± 0·15 s^{-1} (1000 μM)) and deactivation threefold (monoexponential decay time constant: $\alpha1$, 0·22 ± 0·026 s (2 μM); $\alpha3$, 0·68 ± 0·1 s (20 μM)).

5. To gain an insight into the gating mechanisms underlying macroscopic desensitization, we extended a previous gating model of $GABA_A$ receptor single-channel activity to include a desensitization pathway. Such a mechanism reproduced empirical $\alpha1\beta2\gamma2S$ activation, desensitization and deactivation kinetics.

6. To identify molecular transitions underlying the gating differences between $\alpha1\beta2\gamma2S$ and $\alpha3\beta2\gamma2S$ receptors, we explored parameter alterations of the $\alpha1\beta2\gamma2S$ gating model that provided an accounting of $\alpha3\beta2\gamma2S$ empirical responses. Remarkably, alteration of rates and rate constants involved in ligand binding alone allowed reproduction of $\alpha3\beta2\gamma2S$ activation, desensitization and deactivation.

7. These results indicate that substitution of the $\alpha3$ subunit variant in an $\alpha1\beta2\gamma2S$ receptor alters transition rates involved in ligand binding that underlie changes in apparent activating site affinity and macroscopic current gating. Furthermore, they argue strongly that the structural determinants of these functional features reside on the α-subunit.

‡ To whom correspondence should be addressed.

γ-Aminobutyric acid (GABA) is the primary inhibitory neurotransmitter in the vertebrate central nervous system. GABA binding to $GABA_A$ receptors (GABARs) activates an integral chloride channel that generally results in membrane hyperpolarization and suppressed neuronal excitability. These receptors also are modulated by clinically useful drugs such as anxiolytics and anaesthetic agents (Sivilotti & Nistri, 1991).

GABARs are putative heteropentamers involving at least fifteen protein subunits. These subunits are divided into five distinct classes (α, β, γ, δ and ρ) based on amino acid sequence homology where most classes contain multiple variants (reviewed in Seeburg *et al.* 1990; Burt & Kamatchi, 1991). The resultant structural diversity has significance, since the properties of heterologously expressed channels are critically dependent on subunit combination (Levitan 1988; Khrestchatisky *et al.* 1989; Pritchett, Luddens & Seeburg, 1989; Pritchett, Sontheimer, Shivers, Ymer, Kettenmann & Seeburg, 1989; Verdoorn, Draguhn, Ymer, Seeburg & Sakmann, 1990; Draguhn, Verdoorn, Ewert, Seeburg & Sakmann, 1990; Sigel, Baur, Mohler & Malherbe, 1990; Sigel, Baur, Kellenberger & Malherbe, 1992; Angelotti & Macdonald, 1993). The physiological importance of such subunit-dependent function is suggested by anatomical restriction of subunit expression (Wisden, Laurie, Monyer & Seeburg, 1992; Laurie, Seeburg & Wisden, 1992) and functional diversity among native GABA-gated currents (Akaike, Inoue & Krishtal, 1986; Pearce, 1993; Puia, Costa & Vicini, 1994). Therefore, the dependence of gating on subunit composition may represent a critical molecular determinant of synaptic transmission.

The role of component subunits in GABAR function has begun to emerge from functional studies of recombinant receptors. Overall, α, β and γ isoforms are needed to replicate the salient properties of native GABA-gated currents (Levitan *et al.* 1988; Pritchett *et al.* 1989). Here, the β-subunit binds GABA agonists (Casalotti, Stephenson & Barnard, 1986; Deng, Ransom & Olsen, 1986) at receptor sites that trigger channel activation (Amin & Weiss, 1993). The α-subunit also appears involved in channel activation by influencing the apparent affinity of GABA activating sites (Levitan *et al.* 1988; Sigel *et al.* 1990; Sigel *et al.* 1992). In addition, the α-subunit binds benzodiazepines (Fuchs, Mohler & Seighart, 1988; Kirkness & Turner, 1988; Fuchs & Seighart, 1989) triggering enhancement of GABA-gated currents that require the γ-subunit (Pritchett *et al.* 1989).

There are few investigations of subunit-dependent gating. Verdoorn *et al.* (1990) coexpressed $\alpha1\beta2$, $\alpha1\gamma2$ and $\alpha1\beta2\gamma2$ combinations showing that the presence of $\beta2$ enhanced desensitization and outward rectification while $\gamma2$ reduced single-channel mean open time. Angeliotti & Macdonald (1993) coexpressed $\alpha1\beta1$ and $\alpha1\beta1\gamma2S$ subunits and demonstrated that the addition of $\gamma2S$ increased mean open times and burst durations. These studies, while elegant, have contrasted the function between receptors composed of dual and ternary subunit class combinations. To date, only Verdoorn (1994) has examined the role of the α-subunit in a ternary subunit class ($\alpha\beta\gamma$) receptor. Responses triggered by brief (6–25 ms) GABA (3 mM) applications to outside-out macropatches containing $\alpha1\beta2\gamma2$ or $\alpha3\beta2\gamma2$ receptors were studied. Relaxation kinetics were markedly faster for $\alpha1\beta2\gamma2$, suggesting that function influenced by α-subunit subtype plays an important role in determining inhibitory postsynaptic current (IPSC) morphology. However, the details of the underlying function affected by the α-subunit isoform remain unclear.

To this end, we studied whole-cell macroscopic currents of mammalian cells transiently co-transfected with cDNAs encoding either rat brain $\alpha1\beta2\gamma2S$ or $\alpha3\beta2\gamma2S$ GABA subunits. Whole-cell voltage clamp experiments were conducted with single human embryonic kidney (HEK-293) cells using a piezo-actuated two-barrel solution changer (Verdoorn, 1994). This system permitted rapid alterations in extracellular solution (rise time, 30 ms) and allowed the study of macroscopic current kinetics and concentration–response relations during rapidly applied GABA pulses. This approach, which minimizes possible distortion of current kinetics by GABA wash-in (Verdoorn *et al.* 1990), permits characterization of macroscopic current kinetics that is not possible with *Xenopus laevis* oocytes.

We find that substitution of $\alpha3$ for $\alpha1$ reduces the apparent activating site affinity, as previously described in *Xenopus laevis* oocytes (Sigel *et al.* 1990; Sigel *et al.* 1992) and HEK-293 cell (Verdoorn, 1994). Furthermore, this substitution also slows activation, desensitization and deactivation of macroscopic currents. To provide quantitative insight into possible gating mechanisms underlying macroscopic desensitization, we constructed a gating model of the $\alpha1\beta2\gamma2S$ receptor. We extended the gating model of Twyman, Rogers & Macdonald (1990) that accounts for single-channel GABAR activity in murine spinal cord neurons and probable recombinant $\alpha1\beta1\gamma2S$ receptors (Angelotti & Macdonald, 1993). The extended model includes a desensitization pathway and accounted for empirical $\alpha1\beta2\gamma2S$ activation, desensitization and deactivation. To identify possible state transitions influenced by the $\alpha3$ substitution, we considered parameter changes that would allow the $\alpha1\beta2\gamma2S$ model to reproduce the $\alpha3\beta2\gamma2S$ empirical data. Remarkably, only alteration of rates and rate constants involved in ligand binding were required to achieve this goal. These findings indicate that alterations in molecular transition rates involved in ligand binding may underlie discordant activation, desensitization and deactivation kinetics as well as differences in apparent activating site affinity. Furthermore, they argue strongly that the associated structural determinants of these functional features reside on the α-subunit, pointing to a critical role for this isoform in receptor function and synaptic signalling.

METHODS

Cell culture and transient transfection

HEK-293 cells, purchased from the American Type Culture Collection (Bethesda, MD, USA) or generously donated to us by Dr Bruce Stillman, Cold Spring Harbor Laboratory (Cold Spring Harbor, MA, USA), were grown in minimum essential medium (MEM) (Gibco BRL, Grand Island, NY, USA) supplemented with 10% fetal calf serum, 1% glucamine, and 1% penicillin–streptomycin (all Gibco BRL). Cells for experiments were plated onto fibronectin (Sigma)-coated plastic coverslips (Nunc, Inc., Naperville, IL, USA).

During a period of exponential cell growth (1–3 days after plating), the cells can be transfected. Transfection was accomplished with a modified lipofection technique. cDNAs encoding rat brain α1, α3, β2 and γ2S subunits inserted individually into the plasmid pCDM8 (Invitrogen, San Diego, CA, USA) were kindly supplied by Dr Todd Verdoorn, Department of Pharmacology, Vanderbilt University (Nashville, TN, USA). Aliquots of the lipofection reagent (Lipofect amine, Gibco BRL), and appropriate plasmids were mixed in a modified serum-free medium (Optimem, Gibco BRL) and incubated for 10 min. Transfections were based on equal weights of total DNA except for α3β2γ2S combinations where higher expression levels were achieved with a ratio of 2:1:1, respectively. Cells were washed and serum-containing medium was replaced with Optimem and then the liposome–plasmid-containing solution was added to the solution bathing the cells. After a 16–18 h incubation period (37 °C, 5% CO_2), the cells were washed and returned to serum-containing MEM for further incubation under normal conditions (37 °C, 5% CO_2). Cells were ready for electrophysiological studies approximately 48 h after transfection.

Electrophysiology

Coverslips with transfected cells were transferred to a modified culture dish mounted on the stage of an Olympus IMT-2 inverted microscope with Hoffman modulated optics (Olympus, Lake Success, NY, USA). The cells were initially exposed to a modified Tyrode solution containing (mM): 135 NaCl, 5·4 KCl, 1 $MgCl_2$, 5 Hepes (pH 7·2). Before recording currents, the extracellular solution was changed to one in which KCl is replaced by equimolar CsCl. The pipette solution consisted of (mM): 140 CsCl, 1 $MgCl_2$, 11 EGTA, 10 Hepes (pH 7·3). Currents were recorded with whole-cell application of the patch clamp technique (Hamill, Marty, Neher, Sakmann & Sigworth, 1981) using an Axopatch-200 (Axon Instruments) amplifier or a Yale Mark IV amplifier built by us. Data were collected by and stored on IBM-compatible 386 (Dell Computer Corp.) or 486 (Gateway 2000 4DX2-66) computers running the AXOBASIC environment (Axon Instruments) using software of our own design or pCLAMP software (Axon Instruments). We used single cells that were not electrically coupled to other cells as judged by cell capacitance (10 pF, typical for individual HEK cells). Data were collected at room temperature (20–23 °C).

Membrane potential was fixed at −60 mV in all experiments. V_{Cl} (the chloride equilibrium potential) is 0 mV under these ionic conditions. Since GABA-activated channels are Cl^- sensitive (Levitan *et al.* 1988), I_{GABA} were negative (outward Cl^- movement) in our experiments.

GABA application

GABA (Sigma) was applied transiently to the cells via an electromechanical solution changer. Control and test solutions were selected via two separate valves and introduced into both sides of a dual-barrelled pipette. Solution perfusion rate was determined by a syringe pump (Harvard Instruments, Cambridge, MA, USA) and the pipette was positioned grossly via a Narashige hydraulic micromanipulator (Narashige, Greenvale, NY, USA). The pipette was mounted on a macro-block piezoelectric transducer (Polytec Optronics, Costa Mesa, CA, USA) that can move the pipette tip 50 μm in < 5 ms. The cell was continually perfused with control solution. The test GABA-containing solution was applied by delivering the appropriate voltage pulse to the macro-block translator such that the pipette tip moved the distance between the stream centres. In this manner, GABA could be pulsed on/off around a cell in < 30 ms. Test and control solutions could each be changed by selection of one of six separate lines via the control valves. GABA applications were delivered less frequently than every 120 s to prevent accumulation of desensitized receptors.

Parameter estimation and gating model simulation

The parameter estimation technique minimized a squared error performance criterion using the Gauss–Newton method. The algorithm was written in FORTRAN. The performance criterion was defined with a subset of points selected from the target responses such that the general features were reproduced.

Simulations of explicit gating mechanisms were written in Turbo Pascal (Borland International, Scotts Valley, CA, USA) where differential equations were solved numerically using the Euler method. The sensitivity of the response to the iteration time step was examined in all simulations and made sufficiently small to minimize error.

All programs were compiled and executed on an IBM-compatible 486 (Gateway 2000 4DX2-66) computer.

Evaluation of parameter set uniqueness

The uniqueness of parameter sets was evaluated by systematically adjusting the initial parameter values prior to parameter estimation. In this way the performance surface was searched from different initial starting locations. A parameter set was unique if the final parameter values were insensitive to initial values.

Data analysis

Curve fitting, statistics and data analysis were carried out using Origin software (MicroCal, Northampton, MA, USA).

RESULTS

α1β2γ2S and α3β2γ2S receptors manifest distinct properties

Figure 1A compares the responses of expressed α1β2γ2S (left) and α3β2γ2S (right) GABARs to rapidly applied GABA pulses lasting 10 s. In this and all other figures, currents were recorded at a −60 mV holding potential in symmetrical chloride gradients resulting in inward I_{GABA}. These responses reveal distinct functional properties of receptors that have incorporated the different α-subunit subtypes. A 1000 μM pulse applied to a cell expressing α1β2γ2S receptors (left, bottom trace) triggers a characteristic response with rapid activation (downward deflection) that quickly reaches a peak, subsequent slower desensitization, and deactivation. Lower GABA concentrations reduce peak currents and slow current kinetics. The α3β2γ2S response family appears qualitatively similar, but closer examination

reveals quantitative differences. First, the threshold for recording GABA-induced currents is nearly tenfold greater than that for $\alpha1\beta2\gamma2S$ receptors suggesting lower GABA sensitivity for $\alpha3\beta2\gamma2S$ receptors, consistent with previous reports with receptors expressed in *Xenopus* (Sigel *et al.* 1990; Sigel *et al.* 1992) and HEK-293 cells (Verdoorn, 1994). Figure 1*B* plots pooled peak I_{GABA} concentration–response relations for receptors containing both α-subunit variants and confirms the effect of subunit substitution on GABA sensitivity. These relationships, quantitated with Hill equation fits (continuous lines), are both best fitted by curves with Hill coefficients greater than 1 ($\alpha1\beta2\gamma2S$, 1·6; $\alpha3\beta2\gamma2S$, 1·5) suggesting that two bound GABA molecules are required to trigger activation. However, EC_{50} values ($\alpha1\beta2\gamma2S$, 7 μM; $\alpha3\beta2\gamma2S$, 75 μM) differ by tenfold, suggesting a similar lower apparent affinity of GABA binding to $\alpha3\beta2\gamma2S$ receptors.

In addition to apparent receptor affinity, Fig. 1*A* also suggests that the α-subunit subtype may influence desensitization and deactivation kinetics. Receptor channel opening is determined jointly by ligand binding and gating and these processes are mutually influential owing to the physical principle of reciprocity (Edsall & Wyman, 1958). To begin to discern gating kinetics unconfounded by binding, we normalized for differences in apparent affinities by considering I_{GABA} at equi-activating concentrations. This

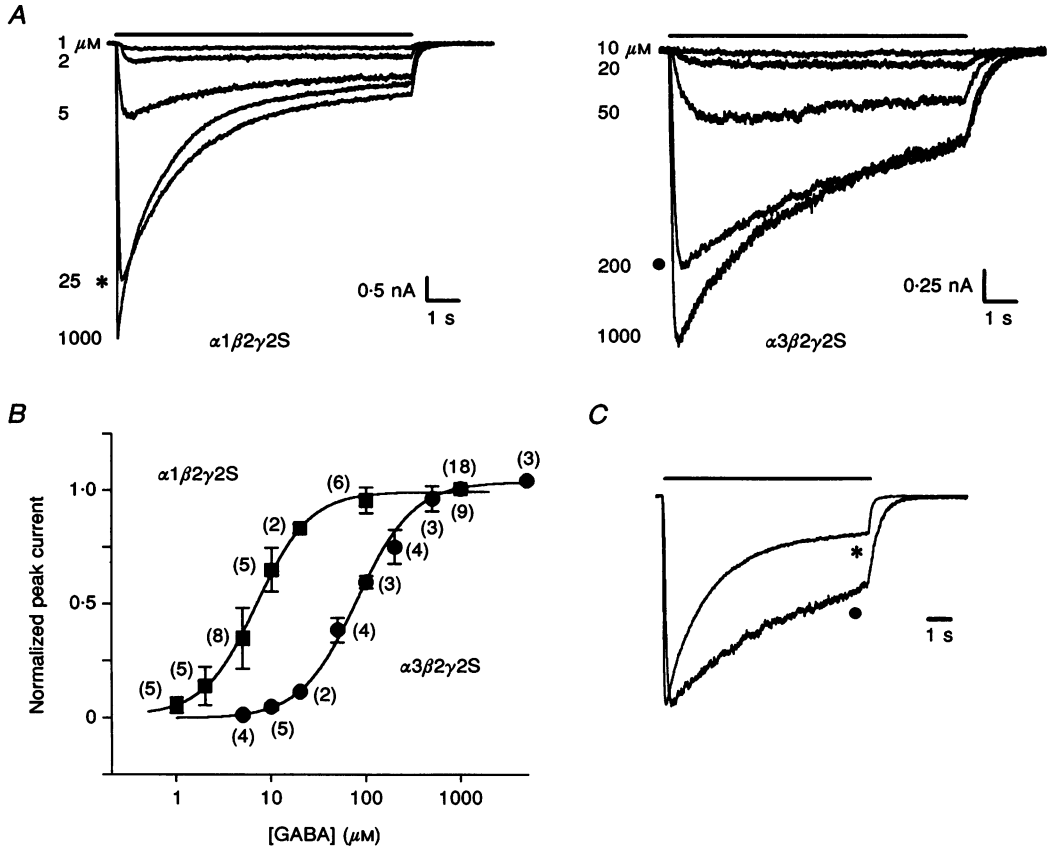

Figure 1. Properties of $\alpha1\beta2\gamma2S$ and $\alpha3\beta2\gamma2S$ receptors: distinctions in kinetics and sensitivity to GABA

A, macroscopic GABA-gated currents (I_{GABA}) recorded at a constant holding potential (−60 mV) under conditions in which $V_{Cl} = 0$ (see Methods) from individual HEK-293 cells expressing $\alpha1\beta2\gamma2S$ (left) or $\alpha3\beta2\gamma2S$ (right) subunits. Shown are current responses to 10 s pulse applications (indicated by bar) over range of GABA concentrations (indicated to the left). GABA-induced currents are inward under these conditions. *B*, concentration–response relations of normalized peak I_{GABA} for cells (mean ± S.D., n in parentheses) expressing $\alpha1\beta2\gamma2S$ and $\alpha3\beta2\gamma2S$ as indicated. Smooth curves are fits of the Hill equation:

$$\text{Normalized peak current} = 1/(1 + EC_{50}/[\text{GABA}]^{n_H}),$$

where EC_{50} is the [GABA] that triggers half-maximal response and n_H is the Hill coefficient, with the following parameters: $\alpha1\beta2\gamma2$, $EC_{50} = 7$ μM and $n_H = 1{\cdot}6$; $\alpha3\beta2\gamma2$, $EC_{50} = 80$ μM and $n_H = 1{\cdot}5$. *C*, I_{GABA} responses at approximately equi-activating GABA concentrations for $\alpha1\beta2\gamma2S$ (25 μM, *) and $\alpha3\beta2\gamma2S$ (200 μM, ●) from Fig. 1*A* normalized to peak current to emphasize kinetic differences.

correction presumes that equi-activating concentrations (based on peak I_{GABA} concentration–response relationships) trigger similar relative peak open probabilities. This allowed us to test whether these observations may be explained by differences in apparent GABA binding alone. Figure 1*C* compares the responses of Fig. 1*A* for $\alpha1\beta2\gamma2S$ and $\alpha3\beta2\gamma2S$ at nearly tenfold different and equi-activating concentrations (25 and 200 μM, respectively). This comparison shows that activation, desensitization and deactivation kinetics are faster when the α1 subtype is present, suggesting that the α-subunit isoform influences transition rates underlying these gating properties. In order to investigate the effects of the α-subtype on gating, we characterized the macroscopic current kinetics over a wide range of GABA concentrations for both receptors.

Activation

Figure 2*A* shows normalized responses from two groups of single cells expressing $\alpha1\beta2\gamma2S$ (left) and $\alpha3\beta2\gamma2S$ (right) receptors to step GABA application at 2 and 20 μM, respectively. The heavy traces are scaled, superimposed responses from three cells. The unscaled data (insets) have different peak amplitudes and demonstrate the range of recombinant channel activity we recorded. This variation is due to differing expression level and cell size. However, activation kinetics are similar because normalization to peak current nearly superimposes these responses. Therefore, expression level, over this range, does not influence gating as has been reported for recombinant potassium channels (Honoré, Attali, Romey, Lesage, Barhanin & Lazdunski, 1992).

Figure 2*B* shows families of mean grouped data over a range of GABA concentrations for both receptors. The fivefold different time scales used for display allow precise identification of peak I_{GABA} but also cause time courses to appear falsely similar. The time of peak I_{GABA} (arrows in Fig. 2*B*), related to the inverse of activation rate, decreases with GABA concentration for both receptors. This yields the expected result that GABA concentration enhances activation. Figure 2*C* plots concentration–response relations of time to peak, where both receptors display an inverse dependence on GABA concentration. However, the time to peak of $\alpha1\beta2\gamma2S$ is greater over the entire concentration range, indicating no overlap of activation rates. This suggests that the range of transition rates underlying receptor activation are dissimilar, where the presence of the α1 subunit speeds activation. These results suggest that molecular transitions underlying activation are influenced by the α-subunit. We next examined desensitization in a similar fashion.

Desensitization

Figure 3*A* shows I_{GABA} desensitization responses, normalized to peak current, from two groups of single cells expressing $\alpha1\beta2\gamma2S$ (left) and $\alpha3\beta2\gamma2S$ (right) at 100 and 1000 μM GABA, respectively. The heavy traces are scaled, superimposed responses from eight (left) and six (right) cells. Unscaled responses (insets) have different peak currents reflecting both variations in expression level and cell size and show the range of expression levels we observed. As for activation kinetics, the time course of desensitization was not sensitive to expression level. It is also apparent that at equi-activating GABA concentration, the $\alpha3\beta2\gamma2S$ receptor manifests slower desensitization.

Figure 3*B* shows families of averaged normalized traces over a range of GABA concentrations for both receptors as indicated. The concentration–response relationship of desensitization kinetics was complex for both receptors. At high GABA concentrations (>100 μM), desensitization was best described by biexponential functions, where the magnitudes of the two component exponentials (slow and fast) as well as their time constants varied with GABA concentration. At low concentrations, desensitization was slow, and well described by a monoexponential. In order to make quantitative comparisons between the concentration dependence of desensitization kinetics for both receptors, we measured the time required to decay to 80% of the peak amplitude (t_{80}, arrows in Fig. 3*B*). The reciprocal of t_{80} is a coarse indicator of desensitization rate. Figure 3*C* gives the concentration–response relationship of this rate for both receptors. Substitution of α1 for α3 shifts this relationship to lower GABA concentrations, as might be predicted from different apparent binding affinities, but also increases maximum rate about threefold with this measure. Increase in maximal rate indicates speeding of desensitization by the α1 subunit and suggests increases in underlying transition rates. Thus, the presence of the α1 subtype enhances desensitization kinetics, similar to activation kinetics.

Deactivation

Figure 4*A* shows I_{GABA} deactivation from two groups of individual cells expressing $\alpha1\beta2\gamma2S$ (left) or $\alpha3\beta2\gamma2S$ (right) observed at the end of a 10 s pulse (2 μM, left and 20 μM, right). The heavy traces are scaled, superimposed responses from four (left) and three (right) cells. Unscaled responses (insets) have different peak currents reflecting both variations in expression level and cell size, but when scaled these responses nearly superimpose. Deactivation kinetics for both receptors were insensitive to concentration (data not shown).

Figure 4*B* compares normalized mean deactivation responses at concentrations for both receptors as indicated. Deactivation is markedly faster in the presence of the α1 subtype where monoexponential time constants were reduced threefold ((means ± S.E.M.): α1, 0·22 ± 0·026 s; α3, 0·68 ± 0·1 s). These results indicate that the transition rates underlying receptor deactivation are influenced by the α-subunit, where the presence of the α1 subtype enhances this process.

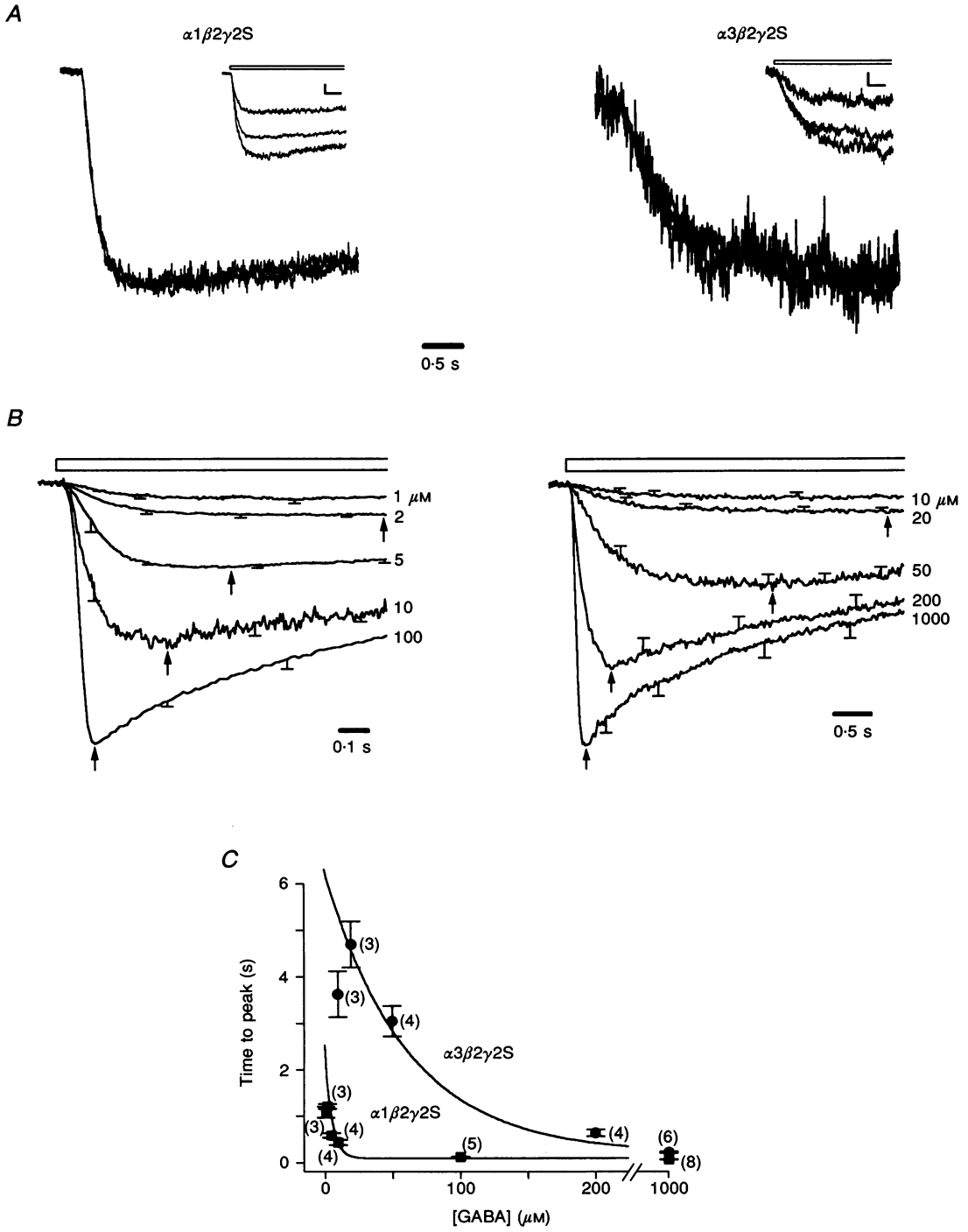

Figure 2. Influence of α-subunit variant on activation kinetics

A, the bold current traces are the superposition of I_{GABA} responses, normalized to peak current, from cells expressing α1β2γ2S (left, $n = 3$) and α3β2γ2S (right, $n = 3$) receptors triggered by 2 and 20 μM GABA step pulses (indicated by open bars in insets), respectively. Insets show individual responses before normalization. Inset scale bars are 0·1 nA and 0·5 s. *B*, means ± S.D. of normalized I_{GABA} responses (values of n are given in Fig. 2*C*) over a range of GABA concentrations (indicated to the right) for cells expressing α1β2γ2S (left) and α3β2γ2S (right) receptors. Time to peak is time from the start of GABA pulse to time of peak current (arrows). GABA application is marked by open bar. *C*, concentration dependence of the time to peak for cells (mean ± S.E.M., n in parentheses) expressing α1β2γ2S and α3β2γ2S receptors; smooth curves drawn by hand.

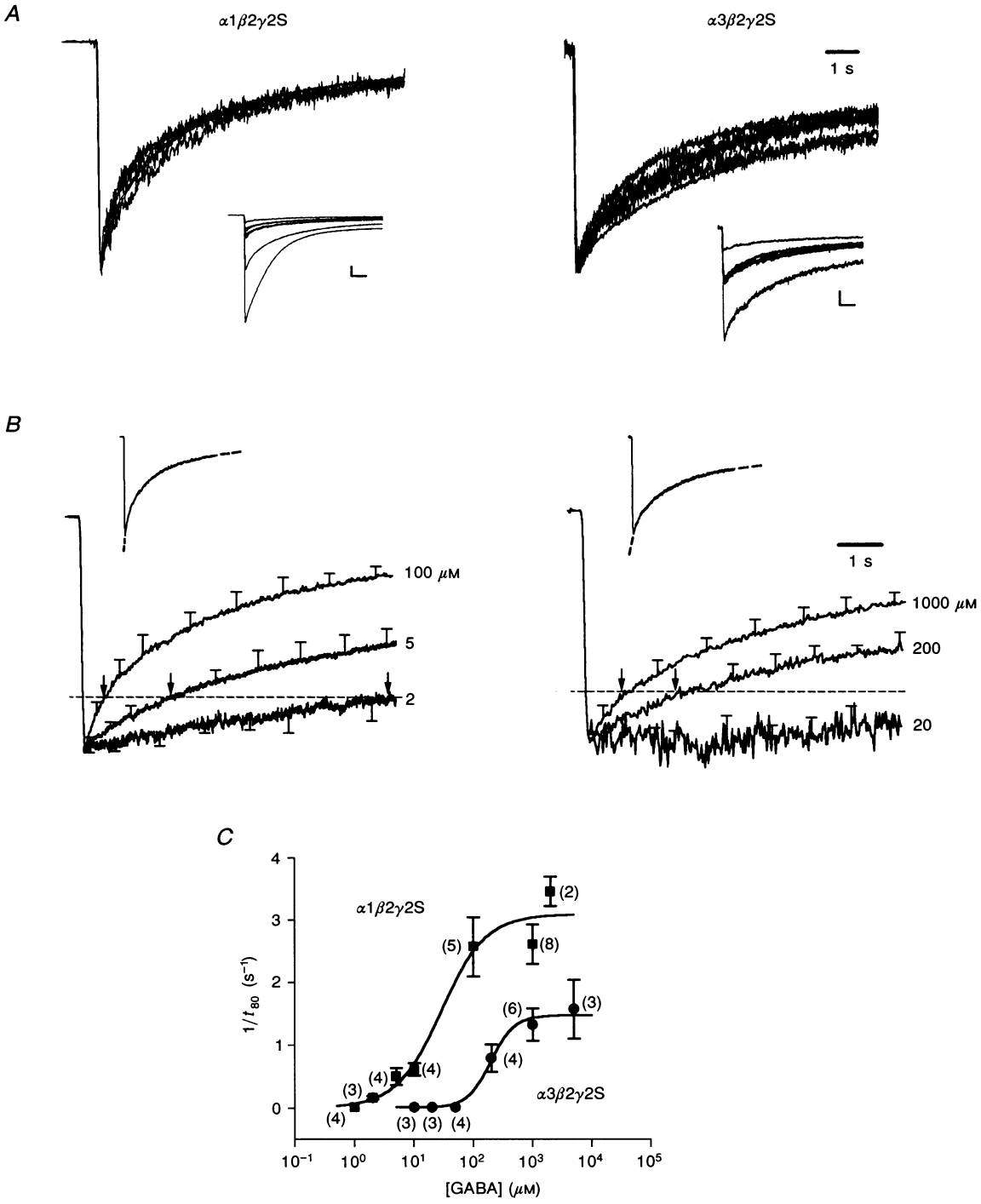

Figure 3. Influence of α-subunit on desensitization kinetics

A, I_{GABA} responses recorded at a slower time base to emphasize kinetics of desensitization. The bold traces show the superposition of responses, normalized to peak current, from cells expressing α1β2γ2S (left, $n = 8$) and α3β2γ2S (right, $n = 6$) receptors triggered by 100 and 1000 μM GABA steps, respectively. The insets show individual responses before normalization (scale bars are 1 nA (left), 0·2 nA (right) with time of 1 s). *B*, the means ± S.D. of normalized responses over a range of GABA concentrations (indicated to the right) are shown for cells expressing α1β2γ2S (left) and α3β2γ2S (right) receptors. These responses were time shifted to align peaks before averaging. Insets show biexponential function fits (dashed lines) to response at highest GABA concentration shown. Arrows indicate the time of current decay to 80% of peak value (dashed line). Time interval between peak current and 80% of peak current is t_{80}. *D*, concentration dependence of the reciprocal of t_{80} for α1β2γ2S and α3β2γ2S receptors (means ± S.E.M., n in parentheses).

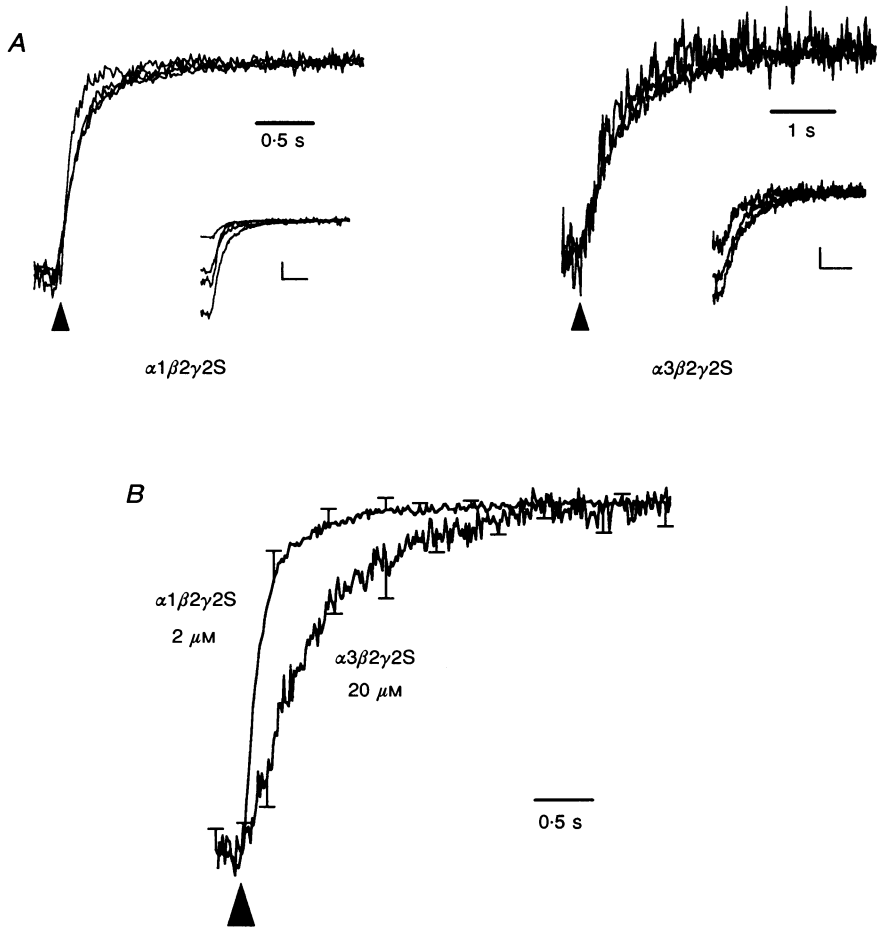

Figure 4. Influence of α-subunit on deactivation

A, bold current traces are the superposition of deactivation I_{GABA} responses, normalized to current at pulse end (arrowheads), from cells expressing $\alpha1\beta2\gamma2S$ (left, $n = 4$) or $\alpha3\beta2\gamma2S$ (right, $n = 3$) receptors triggered by 2 and 20 μM GABA pulses (10 s), respectively. Insets show individual responses before normalization (scale bars: left, 200 pA and 0·5 s; right, 50 pA and 1 s). *B*, normalized mean ± S.D. deactivation responses for $\alpha1\beta2\gamma2S$ and $\alpha3\beta2\gamma2S$ receptors following equi-activating 10 s GABA pulses (concentrations shown). Responses scaled to compare deactivation kinetics.

These results confirm that the α1 subtype increases apparent activating site affinity. Furthermore, they indicate that the presence of α1 subtype speeds activation, desensitization and deactivation kinetics thereby arguing strongly that gating properties are influenced by the α-subunit isoform.

DISCUSSION

GABA binding transition rates account for α-subunit-dependent differences in apparent activating site affinity and gating properties

The empirical results demonstrate that macroscopic current gating is different between the two receptors when normalized for differences in apparent activating site affinities. We wished to understand the molecular underpinnings of the differences in channel function caused by this α-subunit substitution. A comprehensive approach to this question should identify the affected state transitions and provide an insight into how multiple functional effects interact to determine receptor activity observed in macroscopic currents. The former would also be critical in elucidating the structure–function relations for the α-subunit isoform. Our strategy was to construct a gating model that could account for empirical activation, desensitization and deactivation of the $\alpha1\beta2\gamma2S$ receptor. This step would also provide insight into gating mechanisms underlying macroscopic desensitization. With such a mechanism in hand, we could then explore which gating transition(s) could be altered to permit replication of corresponding $\alpha3\beta2\gamma2S$ data. In so doing, candidate molecular transitions influenced by the α-subunit isoform and their interaction could be identified.

In order to construct a detailed gating model, the single-channel properties of GABARs must be considered. The equilibrium single-channel properties of the primary conductance in murine spinal cord neurons are complex (Sakmann, Hamill & Bormann, 1983; Macdonald, Rogers & Twyman, 1989; Weiss & Magleby, 1989; Twyman *et al.* 1990; Twyman & Macdonald, 1992). To account for these observations, an intricate model for the steady-state single-channel activity of the main-conductance state has been developed (Macdonald *et al.* 1989; Twyman *et al.* 1990; Twyman & Macdonald, 1992). We began with the model proposed by Twyman *et al.* (1990). While the gating of recombinant $\alpha1\beta2\gamma2S$ GABARs has not been characterized at the level of single channels, the application of this model to $\alpha1\beta2\gamma2S$ receptors is tenable because of recognized similarities between the single-channel properties of recombinant and neuronal receptors. First, recombinant $\alpha1\beta1\gamma2S$ GABARs, which differ from $\alpha1\beta2\gamma2S$ only in the β-subunit variant, manifest gatings similar to those of murine spinal cord neurons (Angelotti & Macdonald, 1993). Second, expressed $\alpha1\beta2\gamma2S$ GABARs have a 30 pS primary conductance (Verdoorn *et al.* 1990; K. J. Gingrich, W. A. Roberts & R. S. Kass, unpublished observations) that is comparable to $\alpha1\beta1\gamma2$ GABARs (29 pS) and murine spinal cord neurons (27 pS).

The final model (Scheme 1) is identical in form to that of Twyman *et al.* (1990) except for the inclusion of a desensitizing pathway (see below). As modified from Twyman *et al.* (1990), A represents an agonist molecule, C_i represents the ith closed state, and O_i represents ith open state. Parameter values as previously defined (Twyman *et al.* 1990) were (s^{-1}): k_2, 30; k_{-2}, 125; a_1, 1515; b_1, 2·77; a_2, 181; b_2, 12·5; a_3, 32; b_3, 17·5; a'_1, 83; a''_1, 68; b'_1, 5263; b''_1, 323; a'_2, 90; a''_2, 73; b'_2, 5263; b''_2, 323; a'_3, 47; a''_3, 37; b'_3, 5263; and b''_3, 323. These parameter values were held constant, thereby preserving all intraburst and some extraburst neuronal single-channel properties. Also, note that both ligand binding reactions are identical (see Scheme 1). In addition, a sequential two state desensitizing pathway connected to state $2AC_2$ was included, where D_i is the ith desensitized state. The existence of at least two such states is suggested by biexponential desensitization at high GABA concentration (see Fig. 3*B*). This desensitization gating mechanism is also consistent with the proposal of Macdonald & Twyman (1992). The justification for the connection of D_1 to $2AC_2$ is derived from the inability of connections to other states (AC_1, $2AC_3$, $2AO_1$, $2AO_2$ and $2AO_3$) to account for the target empirical data (see below).

In this gating model, the macroscopic current (I_{GABA}) is determined by the time course of the aggregate probability of open receptor conformations (AO_1, $2AO_2$ and $2AO_3$). The model is based on single-channel activity filtered at 1 kHz (3 dB) (Twyman *et al.* 1990), which is a greater dynamic range than that of our whole-cell measurement system (rise time, 30 ms). To approximate the intrinsic filtering of our measurement system and allow comparison of model and macroscopic experimental data, we applied a first order filter (12 Hz, 3 dB) to the model I_{GABA} that approximates a response with a 30 ms rise time.

Six extraburst parameters involved in ligand binding (k_1, k_{-1}) and desensitization (d_1, d_{-1}, d_2, d_{-2}) were estimated to provide an accounting of target empirical data. Estimation of these parameters was simplified by considering a subset of the $\alpha1\beta2\gamma2S$ empirical data. Data were selected if they provided, to a degree, separation of activation, desensitization, or deactivation (Fig. 5). The target data set was completed by including peak current data for responses in Fig. 5 as given in concentration–response curves (Fig. 1*B*). Figure 5 compares average kinetic responses of both receptors at nearly equi-activating GABA concentrations. These comparisons clearly illustrate that activation, desensitization and deactivation kinetics are markedly different between these receptors where gating is accelerated by the presence of the α1 subtype.

The $\alpha1\beta2\gamma2S$ model was first considered without the desensitizing pathway, reducing the number of estimated parameters to two (k_1, k_{-1}). Not surprisingly, no values could be found to account for the target empirical data. The four desensitization parameters (d_1, d_{-1}, d_2, d_{-2}) were then

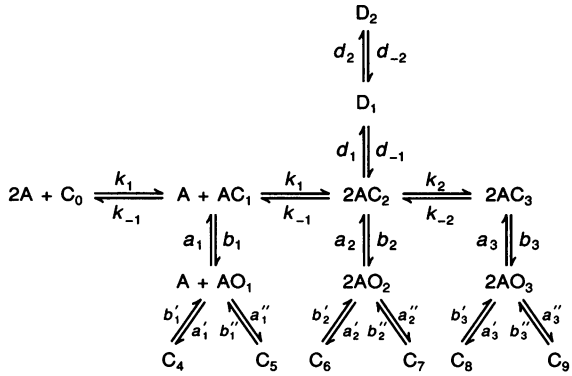

Scheme 1

added and estimation was restricted by fixing the ratio (k_1/k_{-1}) to the empirically observed EC_{50} (7 μM). This reduced the number of free parameters to five. Estimation resulted in parameter values (k_1, 2100 mM^{-1} s^{-1}; k_{-1}, 14·6 s^{-1}; d_1, 30 s^{-1}; d_{-1}, 11·4 s^{-1}; d_2, 0·4 s^{-1}; and d_{-2}, 0·07 s^{-1}) that provided reproduction of the empirical data (Figs 5 and 6*C*, open squares), which enhances the model's validity. The single-channel open probability of this model (0·9% at the end of 1 s, 2 μM pulse) is consistent with that of the model of Twyman *et al.* (1990) (1·9%, 2 μM) suggesting that extraburst behaviour at low concentration was not seriously affected by the introduction of the desensitizing pathway or the small differences in binding parameters (k_1, k_{-1}).

With a credible $\alpha1\beta2\gamma2S$ model in hand, we next considered parameter modifications that would provide reproduction of $\alpha3\beta2\gamma2$ empirical data. Such a process, if successful, would identify molecular transitions that may underlie the gating differences between these structurally similar receptors. This presumes that single-channel properties are not substantially altered by the $\alpha3$ substitution. We first estimated the same parameters (k_1, k_{-1}, d_1, d_{-1}, d_2, d_{-2}) as for $\alpha1\beta2\gamma2S$, but using target empirical data for $\alpha3\beta2\gamma2$ receptor (Figs 1*B* and 5, and EC_{50}, 75 μM). Preliminary parameter estimation revealed that d_1 and d_{-1} agreed closely with the $\alpha1\beta2\gamma2S$ model. We therefore fixed these parameters to those values (d_1, 30 s^{-1}; d_{-1}, 11·4 s^{-1}) and re-estimated k_1, k_{-1}, d_2, and d_{-2}. The final parameters (k_1, 39 mM s^{-1}; k_{-1}, 3 s^{-1}; d_2, 0·31 s^{-1} and d_{-2}, 0·1 s^{-1}) provided a close accounting of the $\alpha3\beta2\gamma2$ empirical data (Figs 5, and 6*C*, open circles). Remarkably, d_2 and d_{-2} values are comparable to those of the $\alpha1\beta2\gamma2$ model (d_2, 0·4 s^{-1}; and d_{-2}, 0·07 s^{-1}), indicating that differences in the two parameters determining binding (k_1 and k_{-1}) alone are nearly sufficient to account for the functional differences in gating and ligand binding. The results indicate that these receptors may differ only in the rates and rate constants that govern state transitions during ligand binding.

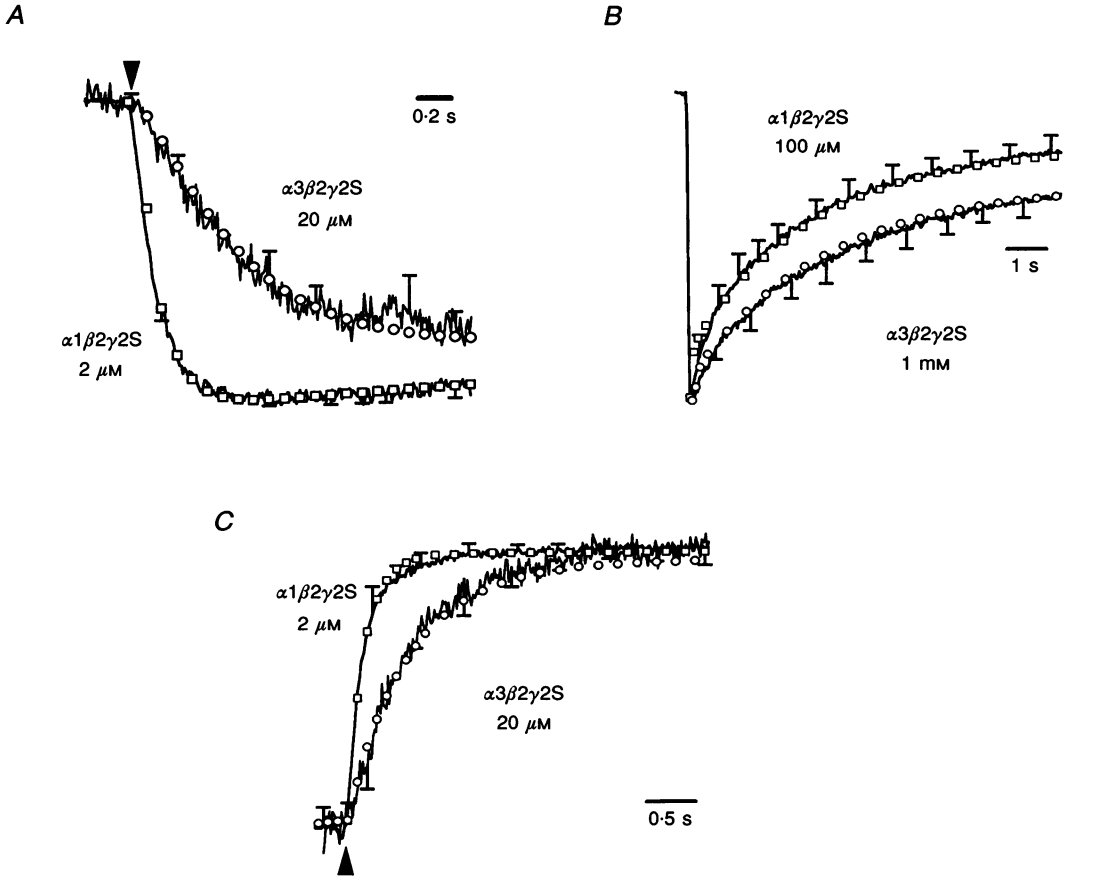

Figure 5. Empirical data used for parameter estimation and resultant gating model responses

The continuous curves are the means ± S.D. of normalized responses (replotted from Figs 2*B*, 3*B* and 4*B*) expressing $\alpha1\beta2\gamma2S$ or $\alpha3\beta2\gamma2S$ subunits, as indicated at equi-activating concentrations. Currents have been scaled to illustrate clearly differing kinetics. Also shown are responses of the gating models ($\alpha1\beta2\gamma2S$, □; $\alpha3\beta2\gamma2S$, ○) for each condition (see text). *A*, step responses (initiation at arrowhead) at low GABA concentration emphasize activation kinetics. *B*, high GABA concentrations enhance desensitization kinetics. *C*, deactivation responses (pulse termination marked by inverted arrowhead).

Model parameters were determined using a subset of empirical data as discussed above. To examine further the validity of these models we tested their ability to predict empirical responses beyond this subset and over a broad range of GABA concentrations. Figure 6 shows the predictions of gating models (open symbols) and empirical data (continuous lines) for both α1β2γ2S and α3β2γ2S receptors. The I_{GABA} traces (Fig. 6*A* and *B*) are normalized

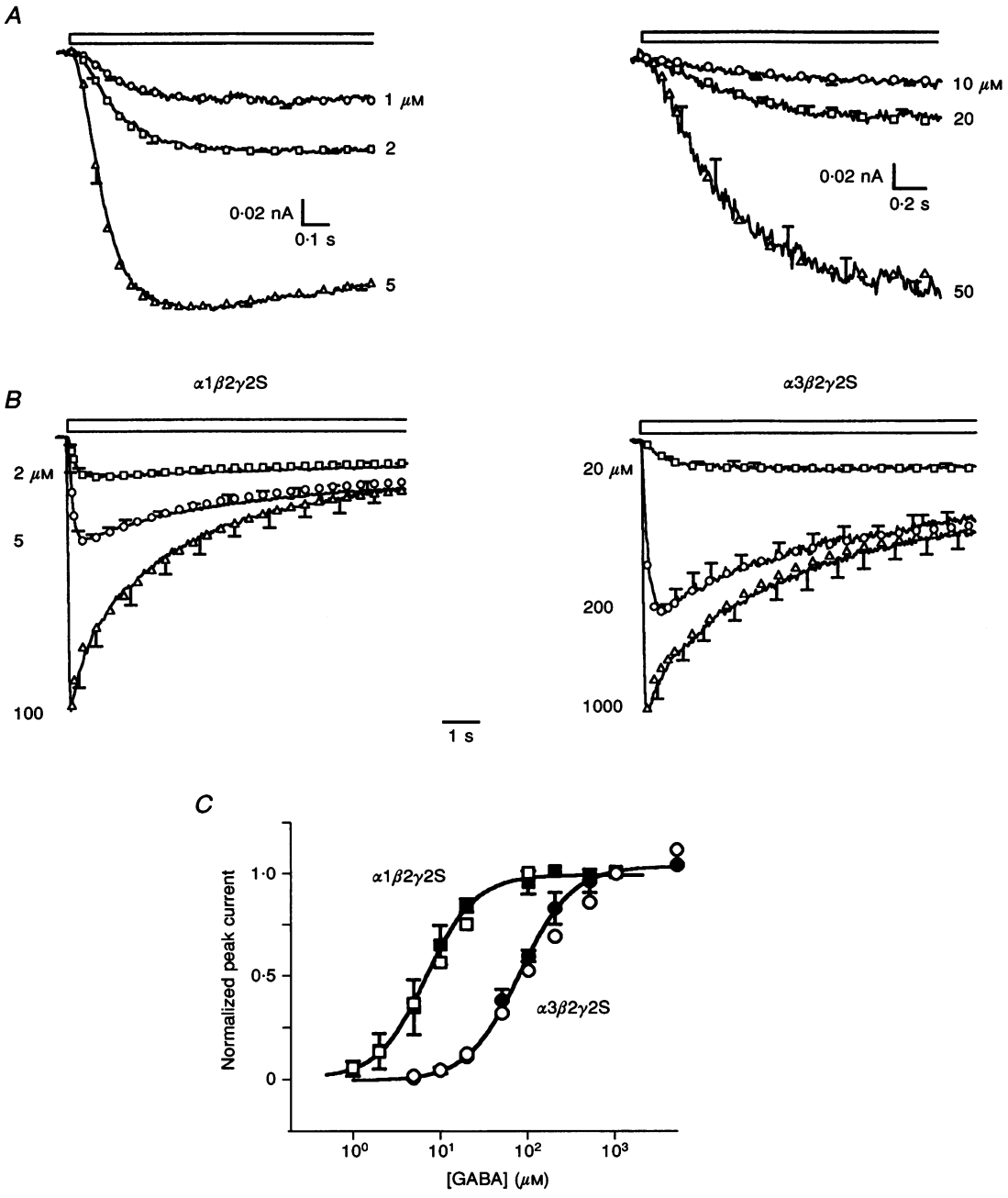

Figure 6. Gating models predictions

In *A* and *B*, gating models predict α-subunit-dependent empirical responses over a broad GABA concentration range (replotted from Figs 2*B* and 3*B*). Empirical data are shown by continuous lines (mean ± S.D.) and GABA concentrations, where appropriate, are shown to the right. Gating model responses (α1β2γ2, □; α3β2γ2, ○) to the same stimulus were scaled to peak current. *A*, activation. Empirical and theoretical responses are shown on an expanded time scale to emphasize activation kinetics during step GABA application (open bar). *B*, desensitization kinetics. Empirical I_{GABA} responses to 10 s GABA (indicated to the left) pulses for cells expressing subunits, as indicated, that are shown on a longer time base to illustrate desensitization kinetics. *C*, concentration–response relationship for peak I_{GABA}. Pooled empirical data are from Fig. 1*B* and gating model data are shown by open symbols.

averaged responses. As shown, the gating models faithfully reproduce the concentration dependence of activation and desensitization kinetics, and peak current amplitude (Fig. 6*C*) of their respective empirical receptors.

Taken together, these results support the validity of the gating models. Furthermore, they suggest strongly that the α-subunit isoform influences transition rates involved in ligand binding that underlie differences both in apparent activating site affinity and macroscopic current gating of the receptor.

α-Subunit isoform contains structural determinants for molecular transitions underlying gating and ligand binding

The principal new result reported here is that the substitution of an α3 for an α1 subunit in an $\alpha1\beta2\gamma2$S GABAR slows the activation, desensitization and deactivation of macroscopic GABA-induced currents in addition to reducing the apparent activating site affinity. Interestingly, our theoretical analysis suggests that effects on both gating and affinity can be accounted for by changes in the molecular transitions governing ligand binding. These findings also indicate that structural determinants for these molecular transitions reside on the α-subunit and point to a critical role of this subunit isoform in receptor function and synaptic signalling. Furthermore, these results lay the foundation for future structure–function studies of the α-subunit isoform in which site-directed mutagenesis can be precisely targeted by exploiting the high degree of amino acid sequence homology between α1 and α3 subunit isoforms (Seeburg *et al.* 1990).

Our approach included a combination of experimental and theoretical elements. We studied macroscopic current kinetics of cells expressing receptors that differed only by the α-subunit subtype ($\alpha1\beta2\gamma2$S and $\alpha3\beta2\gamma2$S), and we comprehensively characterized current kinetics over a wide range of GABA concentrations. We also employed a rapid extracellular solution changer in conjunction with small mammalian cells, minimizing potential distortion of current kinetics by GABA wash-in. Finally, we analysed the empirical data in the context of a comprehensive gating model that accounts for macroscopic gating and is based on GABAR single-channel properties. This step resulted in a gating model that accounts for, or predicts, a wide range of GABAR function and permitted the identification of candidate molecular transitions influenced by the α-subunit.

Involvement of the α-subunit isoform in determining gating of GABARs with a putative native subunit composition ($\alpha\beta\gamma$) is notable. There are few studies that address subunit-dependent gating of GABARs. Angeliotti & Macdonald (1993) found that the addition of γ2 subunits to co-expressed $\alpha1\beta1$ subunits increased mean open time and burst durations. Verdoorn *et al.* (1990) studied $\alpha1\beta2$, $\alpha1\gamma2$ and $\alpha1\beta2\gamma2$ receptors and showed that the presence of β2 enhances desensitization and outward rectification while γ2 reduced mean open time. These important results have shown that gating is dependent on the type and number of subunit classes. Subsequently, Verdoorn (1994) examined the role of the α-subunit in a ternary subunit class receptor ($\alpha\beta\gamma$) by considering the kinetic relaxation of responses triggered by brief (6–25 ms) GABA (3 mM) applications to outside-out macropatches containing $\alpha1\beta2\gamma2$ and $\alpha3\beta2\gamma2$ receptors. Relaxation kinetics were markedly faster for $\alpha1\beta2\gamma2$, suggesting that the functional features that determine inhibitory postsynaptic current morphology are influenced by the α-subunit subtype. However, the underlying functional differences were not identified.

Our results agree with those of Sigel *et al.* (1990, 1992) who have demonstrated that the same α-subunit variant substitution dramatically reduced apparent GABA binding affinity in $\alpha\beta2\gamma2$ subunit combinations expressed in *Xenopus*. In fact, their peak current concentration–response relations ($\alpha1\beta2\gamma2$, $EC_{50} = 6$ and Hill coeffecient = 1·6; $\alpha3\beta2\gamma2$, $EC_{50} = 116$ and Hill coeffecient = 1·3) are quantitatively similar to those of the receptors in this study (see Fig. 1*B*). Likewise, our results are consistent with reports by Verdoorn (1994) of $\alpha1\beta2\gamma2$ ($EC_{50} = 17{\cdot}4\ \mu$M, Hill coeffecient = 1·9) and $\alpha3\beta2\gamma2$ ($EC_{50} = 103\ \mu$M, Hill coefficient = 1·3) expressed in HEK-293 cells. Other reports have implicated the α-subunit in GABA binding of recombinant $\alpha\beta$ receptors (Levitan *et al.* 1988). However, studies of structure–function (Amin & Weiss, 1993) and binding (Casalotti *et al.* 1986; Deng *et al.* 1986) provide good evidence that the β-subunit directly binds GABA to trigger activation. Perhaps the α-subunit indirectly affects β subunit binding of GABA in a manner similar to the probable allosteric influence of the γ-subunit on the α-subunit during benzodiazepine binding (Pritchett *et al.* 1989).

Physiological implications of the gating models

The model

We used a comprehensive reaction scheme (Scheme 1) to account for macroscopic current kinetics. The validity of the resultant models is supported by their reproduction of a wide array of GABAR function, that includes single-channel properties, peak current concentration–response relationships, and macroscopic activation, desensitization and deactivation. However, these findings cannot prove the validity of the model since these functional features do not guarantee a unique model structure. Furthermore, the assumption that the single-channel properties of neuronal and these recombinant receptors are similar must be tested.

This model is unique in its ability to account for a wide range of GABAR function when compared with previous models. Bormann & Clapham (1985) proposed a linear

reaction scheme, based on a model described by del Castillo & Katz (1957) for nicotinic acetylcholine receptors, involving the sequential binding of two agonist molecules that activates to a single open state. This reaction scheme accounted for macroscopic current concentration–response relations, burst durations and closed times of GABA-gated Cl^- channels in adrenal medullary chromaffin cells. Bormann (1988) proposed an extension of this model where singly and doubly bound receptors opened in order to explain the brief openings and burst characteristics of single-channel activity. Later, Twyman *et al.* (1990) proposed the gating model embodied in Scheme 1 to account for three kinetically distinct open states and the concentration independence of intraburst closed times. Our model extends this gating mechanism, by including a desensitization pathway to account for macroscopic current kinetics.

It is interesting to consider this gating model with respect to recent findings by Maconochie, Zempel & Steinbach (1994) of GABAR activation from postnatal cerebellar neurons in rapidly perfused outside-out patches. They found a sigmoidal concentration–response relationship for activation rate. This relationship ($EC_{50} = 500\ \mu M$) was shifted to higher concentration fiftyfold relative to the peak current concentration–response relationship ($EC_{50} = 10\ \mu M$). These observations were accounted for by an activation process where most receptors bind more than one GABA molecule and where the final GABA molecule binds with low affinity. We became interested in examining our model ($\alpha1\beta2\gamma2S$) for these properties since most open channels here also bind two GABA molecules, but in contrast, do so with high affinity. To increase the model's frequency response, we removed the first-order filter. Multi-exponential functions were then fitted to model activation responses over a range of GABA concentrations (Maconochie *et al.* 1994). The model activation rate manifested a sigmoidal dependence on concentration ($EC_{50} = 132\ \mu M$). Surprisingly, this relationship was also shifted to higher concentration nearly twentyfold relative to the current concentration–response relationship ($EC_{50} = 7\ \mu M$). The similarity of these findings suggests that the interpretation of GABAR macroscopic currents may be difficult owing to complex channel gating (Sakmann *et al.* 1983; Macdonald *et al.* 1989; Weiss & Magleby, 1989; Twyman *et al.* 1990; Twyman & Macdonald, 1992) and the interactions of ligand binding and gating.

Predictions for physiologically relevant conditions

Our data show clear kinetic differences for macroscopic currents carried by $\alpha1\beta2\gamma2S$ and $\alpha3\beta2\gamma2S$ GABARs. Do these differences have physiologically relevant implications for receptor function? In order to explore this possibility, we examined the theoretical responses of these receptor types to GABA exposures that may approximate those in the synaptic cleft. These results would provide an insight into the effects of the α-subunit isoform on synaptic transmission.

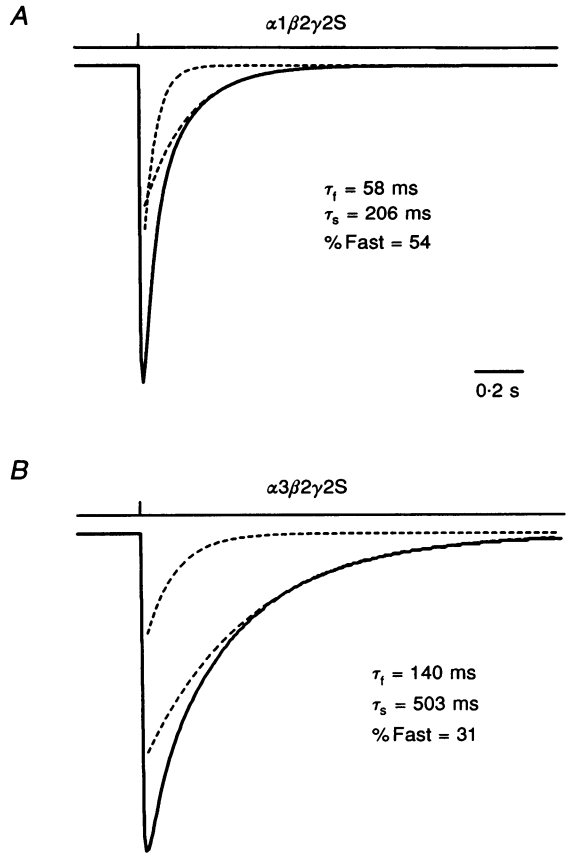

Figure 7. Simulation of physiological inhibitory postsynaptic currents

Model responses (continuous traces) were computed for brief (1 ms) high concentration (1 mM) GABA pulses (upper trace for both panels) to yield simulated inhibitory postsynaptic currents (IPSCs). Responses are normalized to peak current to illustrate differences in relaxation kinetics. Insets give parameters of a fitted biexponential functions (fast time constant (τ_f), slow time constant (τ_s), and percentage of response by fast component (%Fast)). Dashed lines are the time course of the component monoexponentials. Relaxation of $\alpha3\beta2\gamma2S$-simulated IPSC is markedly slower (see text).

The precise time course of cleft neurotransmitter concentration cannot be measured directly. Hence, our current understanding is derived from investigations utilizing a combination of neurotransmitter diffusion modelling and empirical observations of postsynaptic currents at the neuromuscular junction and central synapses (Eccles & Jaeger, 1958; Wathey, Menasche & Lester, 1979; Busch & Sakmann, 1990; Edwards, Konnerth & Sakmann, 1990). Simplifying these conclusions results in a description of the time course of cleft neurotransmitter, as a first approximation, that persists in the order of a millisecond and reaches millimolar concentrations. In our computations, we 'delivered' GABA pulses consistent with this simplification.

Figure 7 shows the response of both gating models to a brief (1 ms) pulse of GABA (1 mM). The shape of these responses is comparable to inhibitory postsynaptic currents (IPSCs) with constant driving force. These responses show divergent qualities where the decay of the $\alpha3\beta2\gamma2$ receptor is markedly slower. Both responses were approximated well by biexponential functions. The presence of the $\alpha3$ subunit slows the overall relaxation time course both by increasing time constants (τ_f, from 58 to 140 ms; τ_s, from 206 to 503 ms) and the relative contribution of the slow component (%Fast: from 54 to 31). Verdoorn (1994) investigated the relaxation of responses triggered by brief (6–25 ms) GABA (3 mM) applications to outside-out macropatches containing $\alpha1\beta2\gamma2$ or $\alpha3\beta2\gamma2$ receptors. The same substitution increased time constants (τ_f, 23 to 40 ms; τ_s, 132 to 546 ms) and the relative contribution of the slow component (%Fast: 62 to 54) which are similar to our theoretical findings.

These results suggest that IPSC morphology may be influenced heavily by transition rates underlying ligand binding and unbinding and that the manner of synaptic transmission may depend heavily on the α-subunit isoform.

From our results we thus conclude that the α-subunit of the $GABA_A$ receptor is critical to molecular transitions involved in GABA binding that influence apparent activating site affinity as well as macroscopic gating. These characteristics are likely to underlie subunit-dependent differences in regional $GABA_A$ receptor function that cause unique postsynaptic inhibitory responses. Future investigations using site-directed mutagenesis can now be undertaken to determine the structural basis for these important physiologically distinct functions.

Akaike, N., Inoue, M. & Krishtal, O. A. (1986). 'Concentration-clamp' study of γ-aminobutyric-acid-induced chloride current kinetics in frog sensory neurones. *Journal of Physiology* **379**, 171–185.

Amin, J. & Weiss, D. S. (1993). $GABA_A$ receptor needs two homologous domains of the beta-subunit for activation by GABA but not by pentobarbital. *Nature* **366**, 565–569.

Angelotti, T. P. & Macdonald, R. L. (1993). Assembly of $GABA_A$ receptor subunits: $\alpha1\beta1$ and $\alpha1\beta1$(gamma)2s subunits produce unique ion channels with dissimilar single-channel properties. *Journal of Neuroscience* **13**, 1429–1440.

Bormann, J. (1988). Electrophysiology of $GABA_A$ and $GABA_B$ receptor subtypes. *Trends in Neurosciences* **11**, 2168–2172.

Bormann, J. & Clapham, D. E. (1985). γ-Aminobutyric acid receptor channels in adrenal chromaffin cells: a patch clamp study. *Proceedings of the National Academy of Sciences of the USA* **82**, 2168–2172.

Burt, D. R. & Kamatchi, G. L. (1991). $GABA_A$ receptor subtypes: from pharmacology to molecular biology. *FASEB Journal* **5**, 2916–2923.

Busch, C. & Sakmann, B. (1990). Synaptic transmission in hippocampal neurons: numerical reconstruction of quantal IPSCs. *Cold Spring Harbor Symposia on Quantitative Biology* **40**, 69–90.

Casalotti, S. O., Stephenson, F. A. & Barnard, E. A. (1986). Separate subunits for agonist and benzodiazepine binding in the γ-aminobutyric $acid_A$ receptor oligomer. *Journal of Biological Chemistry* **261**, 15013–15016.

del Castillo, J. & Katz, B. (1957). Interaction at end-plate receptors between different choline derivatives. *Proceedings of the Royal Society* B **146**, 369–381.

Deng, L., Ransom, R. W. & Olsen, R. W. (1986). [3H]muscimol photolabels the gamma-aminobutyric acid receptor on a peptide distinct from that labeled with benzodiazepines. *Biochemical and Biophysical Research Communications* **138**, 1308–1314.

Draguhn, A., Verdoorn, T. A., Ewert, M., Seeburg, P. H. & Sakmann, B. (1990). Functional and molecular distinction between recombinant rat $GABA_A$ receptor subtypes by Zn^{2+}. *Neuron* **5**, 781–788.

Eccles, J. C. & Jaeger, J. C. (1958). The relationship between the mode of operation and the dimensions of the junctional regions at synapses and motor end-organs. *Proceedings of the Royal Society* B **148**, 38–50.

Edsall, J. T. & Wyman, J. (1958). *Biophysical Chemistry.* Academic Press, New York.

Edwards, F. A., Konnerth, A. & Sakmann, B. (1990). Quantal analysis of inhibitory synaptic transmission in the dentate gyrus of rat hippocampal slices: a patch-clamp study. *Journal of Physiology* **430**, 213–249.

Fuchs, K., Mohler, H. & Seighart, W. (1988). Various proteins from rat brain, specifically and irreversibly labeled by [3H]flunitrazepam, are distinct alpha-subunits of the GABA/benzodiazepine receptor complex. *Neuroscience Letters* **90**, 314–319.

Fuchs, K. & Seighart, W. (1989). Evidence for the existence of several different alpha- and beta-subunits of the GABA/benzodiazepine receptor complex from rat brain. *Neuroscience Letters* **97**, 329–333.

Hamill, O. P., Marty, A., Neher, E., Sakmann, B. & Sigworth, F. J. (1981). Improved patch-clamp techniques for high-resolution current recording from cells and cell-free membrane patches. *Pflügers Archiv* **391**, 85–100.

Honoré, E., Attali, B., Romey, G., Lesage, F., Barhanin, J. & Lazdunski, M. (1992). Different type of K^+ channel current are generated by different levels of a single mRNA. *EMBO Journal* **11**, 2465–2471.

Khrestchatisky, M., MacLennan, A. J., Chiang, M., Xu, W., Jackson, M. B., Brecha, N., Stemini, C., Olsen, R. W. & Tobin, A. J. (1989). A novel α subunit in rat brain $GABA_A$ receptors. *Neuron* **3**, 745–753.

KIRKNESS, E. F. & TURNER, A. J. (1988). Antibodies directed against a nonapeptide sequence of the gamma-aminobutyrate (GABA)/benzodiazepine receptor alpha-subunit. Detection of a distinct alpha-like subunit in pig cerebral cortex but not cerebellum. *Biochemical Journal* **256**, 291–294.

LAURIE, D. J., SEEBURG, P. H. & WISDEN, W. (1992). The distribution of 13 $GABA_A$ receptor subunit mRNAs in the rat brain. II. Olfactory bulb and cerebellum. *Journal of Neuroscience* **12**, 1063–1076.

LEVITAN, E. S., SCHOFIELD, P. R., BURT, D. R., RHEE, L. M., WISDEN, W., KOHLER, M., FUJITA, N., RODRIGUEZ, H. F., STEPHENSON, F. A., PARLISON, M. G., BARNARD, E. A. & SEEBURGH, P. H. (1988). Structural and functional basis for $GABA_A$ receptor heterogeneity. *Nature* **335**, 76–79.

MACDONALD, R. L., ROGERS, C. J. & TWYMAN, R. E. (1989). Kinetic properties of the $GABA_A$ receptor main-conductance state of mouse spinal cord neurons in culture. *Journal of Physiology* **410**, 479–499.

MACDONALD, R. L. & TWYMAN, R. E. (1992). Kinetic properties and regulation of $GABA_A$ receptor channels. In *Ion Channels*, ed. NARAHASHI, T., pp. 315–343. Plenum Press, New York.

MACONOCHIE, D. J., ZEMPEL, J. M. & STEINBACH, J. H. (1994). How quickly can $GABA_A$ receptors open? *Neuron* **12**, 61–71.

PEARCE, R. A. (1993). Physiological evidence for two distinct $GABA_A$ responses in rat hippocampus. *Neuron* **10**, 189–200.

PRITCHETT, D. B., LUDDENS, H. & SEEBURG, P. H. (1989). Type I and type II $GABA_A$-benzodiazepine receptors produced in transfected cells. *Science* **245**, 1389–1392.

PRITCHETT, D. B., SONTHEIMER, H., SHIVERS, B. D., YMER, S., KETTENMANN, H. & SEEBURG, P. H. (1989). Importance of a novel $GABA_A$ receptor subunit for benzodiazepine pharmacology. *Nature* **338**, 582–585.

PUIA, G., COSTA, E. & VICINI, S. (1994). Functional diversity of GABA-activated Cl^- currents in Purkinje *versus* granule neurons in rat cerebellar slices. *Neuron* **12**, 117–126.

SAKMANN, B., HAMILL, O. P. & BORMANN, J. (1983). Patch-clamp measurements of elementary chloride currents activated by the putative inhibitory transmitters GABA and glycine in mammalian spinal neurons. *Journal of Neural Transmission*, suppl. 18, 83–95.

SEEBURG, P. H., WISDEN, W., VERDOORN, T. A., PRICHETT, D. B., WERNER, P., HERB, A., LUDDENS, H., SPRENGEL, K. & SAKMANN, B. (1990). The $GABA_A$ receptor family: Molecular and functional diversity. *Cold Spring Harbor Symposia on Quantitative Biology* **40**, 29–40.

SIGEL, E., BAUR, R., KELLENBERGER, S. & MALHERBE, P. (1992). Point mutations affecting antagonist affinity and agonist dependent gating of $GABA_A$ receptor channels. *EMBO Journal* **11**, 2017–2023.

SIGEL, E., BAUR, R., MOHLER, H. & MALHERBE, P. (1990). The effect of subunit composition of rat brain $GABA_A$ receptors on channel function. *Neuron* **5**, 703–711.

SIVILOTTI, L. & NISTRI, A. (1991). GABA receptor mechanisms in the central nervous system. *Progress in Neurobiology* **36**, 35–92.

TWYMAN, R. E. & MACDONALD, R. L. (1992). Neurosteroid regulation of $GABA_A$ receptor single channel kinetic properties. *Journal of Physiology* **456**, 215–245.

TWYMAN, R. E., ROGERS, C. J. & MACDONALD, R. L. (1990). Intraburst kinetic properties of the $GABA_A$ receptor main conductance state of mouse spinal cord neurones in culture. *Journal of Physiology* **423**, 193–220.

VERDOORN, T. A. (1994). Formation of heteromeric gamma-aminobutyric acid type A receptors containing two different alpha subunits. *Molecular Pharmacology* **45**, 475–480.

VERDOORN, T. A., DRAGUHN, A., YMER, S., SEEBURG, P. H. & SAKMANN, B. (1990). Functional properties of recombinant rat $GABA_A$ receptors depend on subunit composition. *Neuron* **4**, 919–928.

WATHEY, J. C., MENASCHE, M. N. & LESTER, H. A. (1979). Numerical reconstruction of the quantal event at nicotinic synapses. *Biophysical Journal* **27**, 145–164.

WEISS, D. S. & MAGLEBY, K. (1989). Gating scheme for single GABA-activated Cl^- channels determined from stability plots, dwell-time distributions and adjacent interval analysis. *Journal of Neuroscience* **9**, 1314–1324.

WISDEN, W., LAURIE, D. J., MONYER, H. & SEEBURG, P. H. (1992). The distribution of 13 $GABA_A$ receptor subunit mRNAs in the rat brain I. telencephalon, diencephalon, mesencephalon. *Journal of Neuroscience* **12**, 1040–1062.

Received 21 September 1994; accepted 15 June 1995.